

MORSE POTENTIAL AS A SEMICONDUCTOR QUANTUM WELLS PROFILE

VALENTINA MARTÍNEZ RENDÓN¹

CAROLINA CASTAÑO URIBE¹

ANDREA GIRALDO MARTÍNEZ¹

JUAN PABLO GONZÁLEZ PEREIRA¹

 RICARDO LEÓN RESTREPO ARANGO¹

ÁLVARO LUIS MORALES ARAMBURO²

CARLOS ALBERTO DUQUE ECHEVERRI²

ABSTRACT

This paper presents theoretical calculations of the energy and wave function of the ground state and the first excited state of an electron confined in a GaAsAl/GaAs quantum well with a Morse potential profile using the effective mass approximation method and the envelope wave function. The intersubband transitions are analyzed according to the parameters that define the geometry of the Morse potential to represent the interdiffusion between materials of the barrier and the well. In addition, the peaks of the nonlinear optical rectification are shown as a function of energy of incident photons and their resonance with the transition energy between the two states. An electric field in the growth direction of the quantum well and a magnetic field perpendicular to the heterostructure are applied in order to study the shifts in the optical response peaks in the spectrum of the incident photons.

KEYWORDS: Quantum well, Morse potential, electric field, magnetic field, nonlinear optical rectification.

POTENCIAL DE MORSE COMO PERFIL DE POZOS CUÁNTICOS SEMICONDUCTORES

RESUMEN

Se presentan los cálculos teóricos de la energía y la función de onda del estado base y primer estado excitado de un electrón confinado en un pozo cuántico de GaAsAl/GaAs con perfil de potencial tipo Morse usando la aproximación de masa efectiva y el método de función de onda envolvente. Se analizan las transiciones inter-sub-banda de acuerdo a los parámetros que definen la geometría del potencial de Morse para representar la inter-difusión entre los materiales de la barrera y del pozo. Adicionalmente, se presentan los picos de la rectificación óptica no lineal en función de la energía de los fotones incidentes y su resonancia con la energía de transición entre los dos estados. Se aplica un campo eléctrico

¹ Universidad EIA, Envigado, Colombia

² Condensed Matter Group-UdeA (Grupo de Materia Condensada-UdeA), Physics Institute, Natural Sciences Faculty, Universidad de Antioquia-UdeA, Medellín, Colombia



Correspondence author: Restrepo-Arango, R.L. (Ricardo León): Universidad EIA, Sede de Las Palmas: Km 2 + 200 Vía al Aeropuerto José María Córdova, Envigado, Colombia. Código Postal: 055428 / Tel: (574) 549090 Ext. 361 Email: pfire@eia.edu.co

Paper history:

Paper received on: 20-XI-2015 / Approved: 30-III-2016

Available online: May 30 2016

Open discussion until May 2017

en la dirección de crecimiento del pozo cuántico y un campo magnético perpendicular a la heteroestructura con el fin de estudiar los corrimientos de los picos de la respuesta óptica en el espectro de los fotones incidentes.

PALABRAS CLAVE: pozo cuántico, potencial de Morse, campo eléctrico, campo magnético, rectificación óptica no lineal.

POTENCIAL MORSE COMO PERFIL DE POÇOS QUÂNTICOS SEMICONDUTORES

RESUMO

Se apresentam os Cálculos teóricos da energia e a função da onda do estado fundamental eo primeiro estado excitado de um elétron confinado em um poço quântico GaAsAl/GaAs com perfil de potencial tipo Morse usando a aproximação da massa efetiva e o método da função de onda envolvente. Se analisa as transições enter-sub-banda de acordo com os parâmetros que definem a geometria do potencial de Morse, para representar a Inter difusão entre os materiais de barreira e do poço. Além disso, se apresentam os picos da retificação óptica não linear em função da energia dos fotões incidentes e sua ressonância com a energia de transição entre os dois estados. Se aplica um campo eléctrico na direção do crescimento de poço quântico e um campo magnético perpendicular à heterostrutura, a fim de estudar os desvios dos picos da resposta óptica no espectro dos fotões incidentes.

PALAVRAS-CHAVE: Poços quânticos; Potencial de Morse, Campo eléctrico, Campo magnético, Retificação óptica não linear.

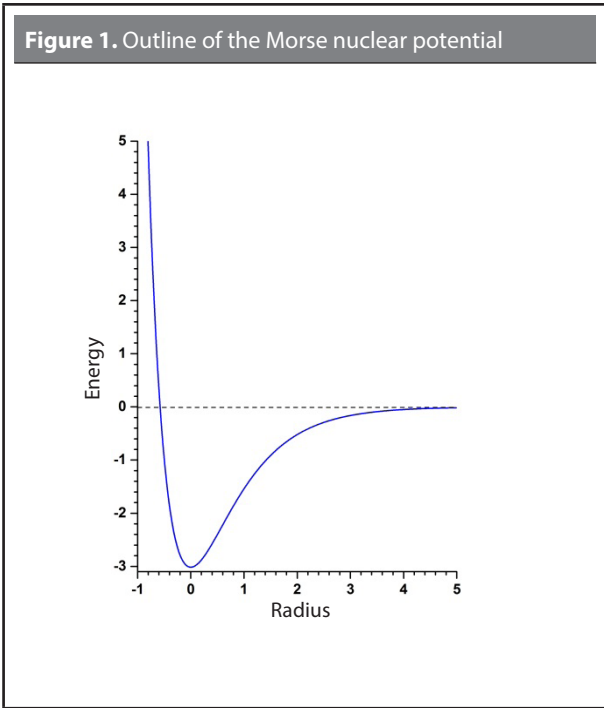
1. INTRODUCTION

There is considerable interest in optical phenomena based on intersubband transitions in low-dimensional semiconductor quantum systems. This is mainly due to the quantum confinement effect, which allows for higher values of the dipole matrix elements and the possibility of achieving resonance given the conditions that allow for those confinements. Both linear and nonlinear optical processes in these semiconductor structures have been studied by various authors in different low-dimensional systems; see, for example, Keshavarz *et al.* (2010), Baskoutas *et al.* (2011), Ungan *et al.* (2011), Barseghyan *et al.* (2012), and Duque *et al.* (2012). Since two states connect in the dipole matrix elements in a closed cycle, we must guarantee that its product is not zero. This only occurs if the states are of mixed parity, which is due to the non-symmetrical potentials. A well-known example of such an asymmetrical potential is the Morse potential, see **Figure 1**. Castro *et al.* (2006), Ikhdaïr (2009), and the precursor Gurnick *et al.* (1983) show and analyze the effects of this type of confinement on the energy of the carriers, the transitions between states, and the associated properties.

Current quantum well growth techniques that graduate the concentration of aluminum allow us to experimentally obtain an infinite number of semiconductor heterostructures with asymmetrical profiles. Some of them or a combination of them could take on the geometric shape of the Morse potential. It is clear that there are restrictions on the stoichiometry; in the case of GaAs-GaAlAs, the maximum concentration of aluminum that is used to maintain a direct energy gap system—with a maximum of the valence band and a minimum of the conduction band in the center of the first Brillouin zone—is $x = 0.35$. The infinite barrier in the Morse potential can be interpreted as a semiconductor/vacuum interface.

In addition, it is well known that the nonlinear optical properties of semiconductor quantum wells generally and mainly depend on the asymmetry of the confinement potential. This asymmetry in the potential profile can be obtained, for example, either through application of an electric field to a symmetrical quantum well or through stoichiometry of the elements used to make semiconductor quantum wells. In this sense, various articles have been published on the theoretical analysis of the second- and third-order linear and

nonlinear optical properties in asymmetrical quantum wells, including Guo *et al.* (2013), Ugan *et al.* (2014 and 2015).



Experimental studies on linear and nonlinear optical properties associated with intersubband transitions in semiconductor quantum heterostructures have been reported by different authors, for example: Unterrainer *et al.* (1996), Vodopyanov *et al.* (1997, 2008), Larrabee *et al.* (2002), Nakai *et al.* (2004), and Lee *et al.* (2014).

Nonlinear optical rectification in asymmetrical quantum wells and the effects of the quantum well size and the influence of external fields as control parameters for this nonlinear optical property have been recently studied by various authors. See Xie (2014), Kumar *et al.* (2014), Hayrapetyan *et al.* (2015), and Shojaei *et al.* (2015). We recommend the articles by Zhang *et al.* (2007), Hargreaves *et al.* (2009), Rowley *et al.* (2012) to understand the experimental processes that present measures associated with optical rectification.

The article by Bhattacharya & Mi (2007) and the citations included in it are a review of the applications of these systems based on semiconductor quantum nanostructures given their electronic and optical properties. Some of them are being used in lasers, infrared

detectors, optical amplifiers, light emitting surfaces, LEDs, and other optoelectronic devices.

The goal of this article is to present the energy and wave function results of the first two states of an electron in a GaAsAl/GaAs quantum well with Morse potential, and to analyze the intersubband transitions and their dependence on the parameters that define the geometrical confinement and the effects of the electric and magnetic field. The article finally shows the influence of these agents on the position and amplitude of the peaks on the nonlinear optical rectification.

2. THEORETICAL MODEL

This article presents the effects of electric and magnetic fields on the energy of the first two states of an electron in a GaAs/Ga_{1-x}Al_xAs quantum well with Morse potential that is grown along the z-axis. The theoretical focus uses the effective mass approach and the envelope wave function technique.

The electric field is chosen along the growth direction of the quantum well ($F = F\hat{z}$). The magnetic field is oriented in the x direction: $B = B\hat{x}$; for the potential vector $\vec{A}(\vec{r})$, the Landau calibration is considered so that $\vec{A}(\vec{r}) = (0, -Bz, 0)$.

Therefore, the Hamiltonian for an electron confined in a quantum well is given by:

$$H = \frac{1}{2m^*} \left(\vec{P} + \frac{e}{c} \vec{A}(\vec{r}) \right)^2 + V_M(z, \gamma) + eFz \quad (1)$$

where $m^* = 0,067 m_0$ is the effective mass of the electron in the gallium arsenide and m_0 is the mass of the free electron, \vec{P} is the linear momentum operator, e is the absolute value of the electron's charge, c is the speed of light in a vacuum, F is the electric field magnitude, and $V_M(z, \gamma)$ is the Morse confinement potential described below. In nuclear physics, Morse potential is usually used to describe the interaction of the atoms that form diatomic molecules. According to Gurnick *et al.* (1983), this potential can be represented as:

$$V_M(r, \gamma) = D_e (1 - e^{-\gamma r})^2 \quad (2)$$

where D_e is known as the dislocation potential of the molecule or depth of the potential well, r is the intermolecular distance, and γ is the parameter that

controls the well's width. The Morse potential used for this study is:

$$V_M(z, \gamma) = V_0(x) (1 + e^{-2\gamma z} - 2e^{-\gamma z}) \quad (3)$$

with γ varying in steps of 0.05 nm^{-1} between 0.05 nm^{-1} and 0.35 nm^{-1} . The height of the right potential barrier $V_0(x)$ (with $F=0$ and $B=0$) has dependence on the concentration of aluminum x according to Lee *et al.* (1980):

$$V_0(x) = 0,6 (1115x + 370x^2) \text{ meV} \quad (4)$$

To obtain the wave functions of an electron corresponding to the Morse potential states, a method developed by Xia and Fan (1989) is used. This focus is based on the expansion of the electronic states on a complete orthogonal base of sine functions associated with a quantum well with infinitely wide potential barriers $L_\infty = 40 \text{ nm}$. The wave functions themselves which depend on z and satisfy the Hamiltonian presented in **Equation (1)** are:

$$\varphi(z) = \sqrt{\frac{2}{L_\infty}} \sum_{m=1}^{\infty} C_m \sin\left(\frac{m\pi z}{L_\infty} + \frac{m\pi}{2}\right) \quad (5)$$

Of course, the number of terms included in the calculation cannot be infinite. The convergence of **Equation (5)**, for the specific size of the quantum well being considered, is guaranteed by the incorporation of 50 terms in the expansion of the wave functions.

In quantum well systems, the possibility of tuning the spectrum of energy levels can be achieved through geometrical configuration of the well or of the stoichiometric conditions of the barriers. This can lead to an almost homogenous distribution of energy differences between the states. The expressions which allow us to calculate the coefficients corresponding to the nonlinear optical rectification for the transitions between the energies of the two calculated states are considered according to Rosencher & Bois (1991):

$$\chi_0^{(2)} = \frac{4e^3 \rho_{01}}{\varepsilon_0 \hbar^2} M_{01}^2 \Delta_{01} \frac{\omega_{01}^2 \left(1 + \frac{\tau_1}{\tau_2}\right) + \left(\omega^2 + \frac{1}{\tau_2^2} \left(\frac{\tau_1}{\tau_2} - 1\right)\right)}{\left(\omega_{01}^2 - \omega^2 + \frac{1}{\tau_2^2}\right) \left(\omega_{01}^2 + \omega^2 + \frac{1}{\tau_2^2}\right)} \quad (6)$$

The parameters used in this equation are defined as follows: ε_0 is the vacuum permittivity, ρ_{01} is the electronic density, \hbar is the Planck constant, for the incident radiation along the z direction we have $M_{ij} = \langle \varphi_i | e z | \varphi_j \rangle$

as the dipole matrix elements with $(i, j = 0, 1)$ and $\Delta_{01} = |M_{00} - M_{11}|$, ω as the frequency of the incident photons, $\omega_{01} = \Delta E_{10} / \hbar$ is the transition frequency with $\Delta E_{10} = E_1 - E_0$ and the terms τ_k with $k = (1, 2)$ are associated to the half-life of the states that participate in the transitions.

The following section presents the results for the energy and the wave functions of the electron's basic state and the first excited state as a function of the width of the quantum well. It also considers the potential profile for different values of the width parameter γ of the Morse potential well, simultaneously considering different values for the electric field or the magnetic field, as well as the nonlinear optical rectification coefficients for such configurations.

3. RESULTS AND DISCUSSION

In addition to the known quantities \hbar , e , ε_0 and c , the following parameters were considered for the calculations in this article: $V_0(x = 0.35) = 261,5 \text{ meV}$, $\rho_{10} = 3.8 \times 10^{23} \text{ m}^{-3}$, $\tau_1 = 1 \text{ ps}$, $\tau_2 = 0.2 \text{ ps}$.

Figure 2 shows the representative outlines of the energies and the squares of the wave functions for the first two states of an electron and the respective Morse confinement potential profile for values of $\gamma = 0,05 \text{ nm}^{-1}$ in **Figure 2a** and $\gamma = 0,15 \text{ nm}^{-1}$ in **Figure 2b**. In this figure, we can see the effect of parameter γ on the asymmetrical geometry of the confinement profile since the electric and magnetic fields have not been considered for them. As can be seen for $\gamma = 0,05 \text{ nm}^{-1}$ in **Figure 2a**, there is a well width of $w \approx 22 \text{ nm}$ and a transition energy between the states of $\Delta E_{10} \approx 40 \text{ meV}$ while in **Figure 2b** with $\gamma = 0,05 \text{ nm}^{-1}$, the values for these quantities are $w \approx 14 \text{ nm}$ and $\Delta E_{10} \approx 100 \text{ meV}$. The wider the well, the lesser the confinement, and the energies are lower than in cases of greater confinement. This is due to the functional form of the Morse potential that appears in **Equation (3)**. The effect on the squares of the wave functions is also noteworthy: the basic state with a central maximum and a first excited state with two maximums that occupy the region of the well width are more extended and have a lesser height in **Figure 2a** than in **Figure 2b**, where the maximums have a greater height and are closer for the second state. We can again see the asymmetry in the probability density of the electronic wave functions. This behavior is an indicator that

the confinement due to the chosen potential favors the dipole matrix elements not tending toward very small values, that is, not reaching zero, thereby allowing for nonlinear optical rectification of the proposed system. On the (blue) curve that represents the confinement potential profile, we can see the asymmetry between the barriers on the left and the right. In the case of **Figure 2b**, the barriers have a more vertically pronounced slope and greater height than in **Figure 2a**. The height of the barriers determines the repulsion on wave functions of the electron toward the center of the heterostructure, reinforcing the confinement and the increase in energy in each state.

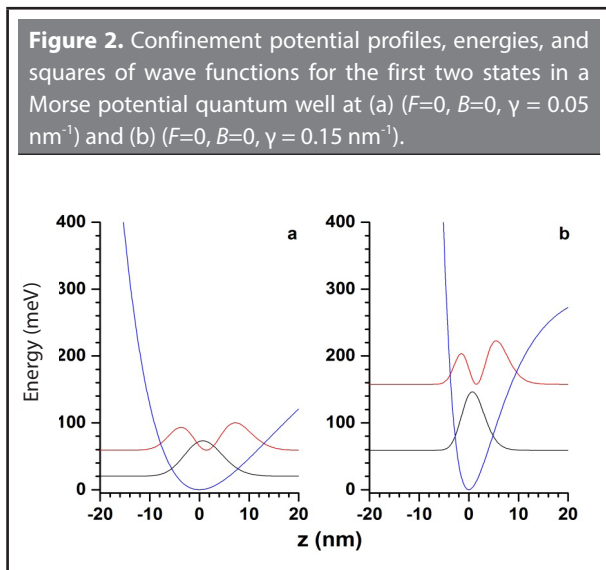


Figure 3 shows the same physical quantities for the system, but now setting parameter $\gamma = 0,05 \text{ nm}^{-1}$ and varying the electrostatic field. **Figure 3a** takes a field that is antiparallel to the growth direction of the quantum field (right to left) with a value of $F_1 = -40 \text{ kV/cm}$, and in **Figure 3b**, the electric field in the growth direction (left to right) of the quantum field has a value of $F_2 = 40 \text{ kV/cm}$. If we compare both figures with **Figure 2b** where $F=0$, we can observe that the electric field contributes more to the asymmetry of the confinement profile. This is important to note since in the beginning, the Morse potential quantum well with an electrical field applied is a non-center symmetrical heterostructure (the maximums of the wave functions are delocalized from the point $z = 0$). This behavior can be understood through the shape and height of the right-side barrier in

Figures 3a and **3b**. For negative field F_1 the well width tends toward $w \approx 26 \text{ nm}$ and for positive field F_2 it tends toward $w \approx 20 \text{ nm}$. This causes the values of the energies for the basic state and first excited state, as well as the energy transition between them, to be greater for the case of the positive electric fields when compared with these values with negative fields.

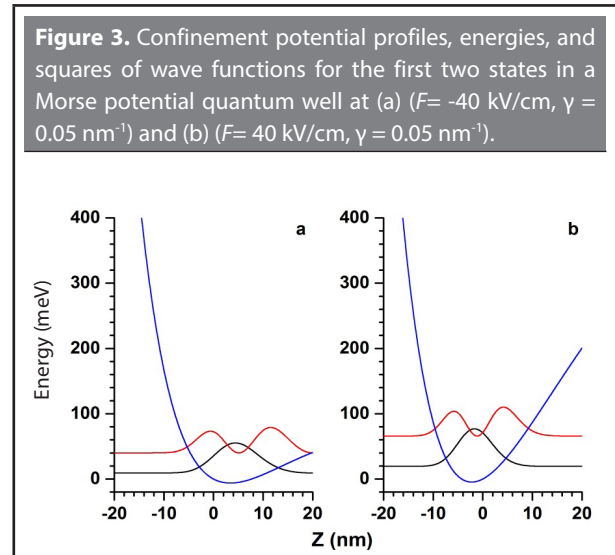


Figure 4 presents $\gamma = 0.15 \text{ nm}^{-1}$, where the electric field values are kept the same as those in **Figure 3**, that is, $F_1 = -40 \text{ kV/cm}$ in **Figure 4a** and the parallel electric field $F_2 = 40 \text{ kV/cm}$ in **Figure 4b**. On these curves, the behavior described in **Figure 3** is even more pronounced because the effect of parameter γ and the chosen electric fields accentuate the asymmetry of the confinement profile. When compared to **Figure 3**, the increase in the individual energy levels and the transition energy levels is nearly 3 times greater in the case of those labeled (a) and 2.5 times greater than those shown in (b). The narrowing of the probability density and the differences in the right barrier between **Figures 4a** and **4b** favor the high degree of confinement and, although the asymmetry of the second state is maintained, the maximums are now back at the point $z = 0$. There are still large differences between **Figures 3** and **4** in the expected values for the dipole matrix elements $M_{ij} = \langle \varphi_i | e z | \varphi_j \rangle$.

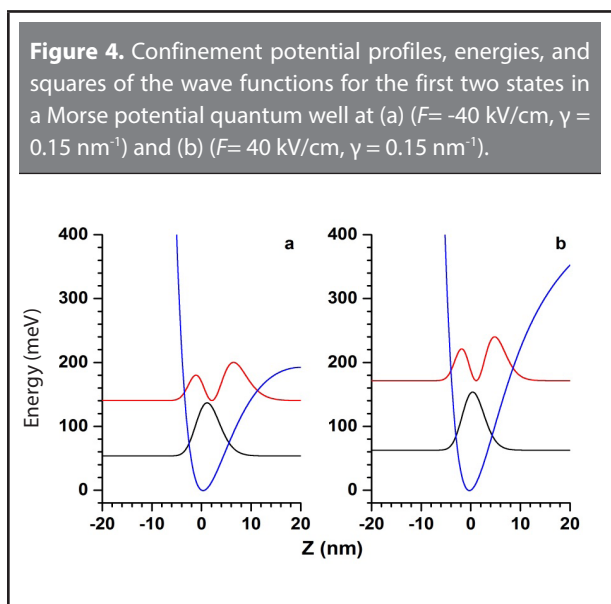
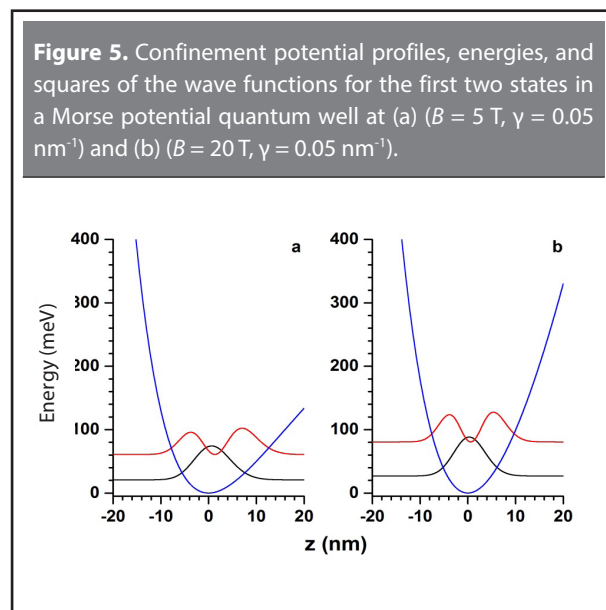


Figure 5 shows the energies and the squares of the wave functions for the two lower states of an electron, as well as the Morse potential profile in a quantum well with $\gamma = 0.05$ nm⁻¹ and $F = 0$. **Figure 5a** corresponds to a magnetic field $B_1 = 5$ T, and **Figure 5b** to $B_2 = 20$ T. Using **Figure 2a** as a reference, we can see that when the magnetic field magnitude increases, the energy of the states increases, and the transition energy increases from 40 meV in 5a to 58 meV in 5b. This is due to the fact that a greater magnetic field changes the well's Morse asymmetry into a profile that tends toward a parabolic shape, and the effective width of the well decreases, producing greater confinement of the charge carriers. We can see that the right barrier's height increases as the magnetic field does the same. This moves the electronic wave functions slightly to the left side of the quantum well. It is important to highlight the fact that the growing magnitude of the magnetic field makes the values of the dipole matrix elements decrease their absolute value.

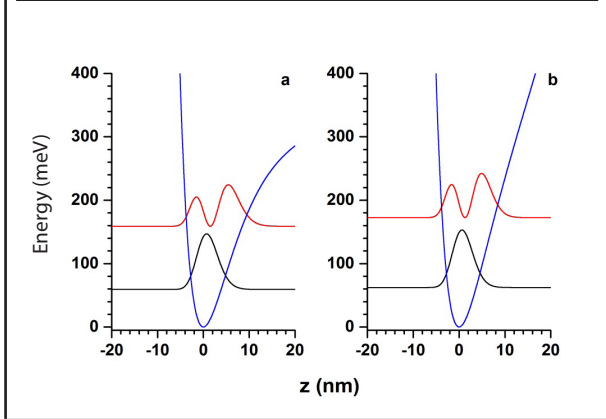
Figure 6 shows the same physical quantities but for Morse quantum wells with parameter $\gamma = 0.15$ nm⁻¹, which is the parameter that defines the effective width of the quantum well, the asymmetry of the barrier height, and the probability density of the wave functions. The same values for the magnetic field in **Figure 6a** with $B_1 = 5$ T and **Figure 6b** with $B_2 = 20$ T are considered here. When compared to **Figure 6**, we

can observe that the combination of parameter γ and the magnetic field produce greater confinement with they both increase, emphasizing the asymmetry of the semiconductor heterostructure. We can observe the considerable increase of the values of the energy of the states and the transition energy. This effect also makes the potential barriers higher than in all the cases presented above, and therefore the confinement of the electrons is greater. This decreases the value expected for the dipole matrix elements.



Once the electronic structure has been obtained, we calculate the dipole matrix elements necessary for calculating the nonlinear optical rectification. For this property in particular, the most relevant matrix element M_{10} was used, as well as the difference in transition energy ΔE_{10} . These give us the frequencies ω_{01} which, when resonating with the frequency of the incident photons, produced a spike in the optical response. In this quantum system, due to the asymmetry of the Morse potential profiles and the effects of the electric and magnetic fields, we find that the difference of dipole matrix elements is not zero, that is, the terms $\Delta_{01} \neq 0$ and this contributes to the magnitude of the nonlinear optical rectification.

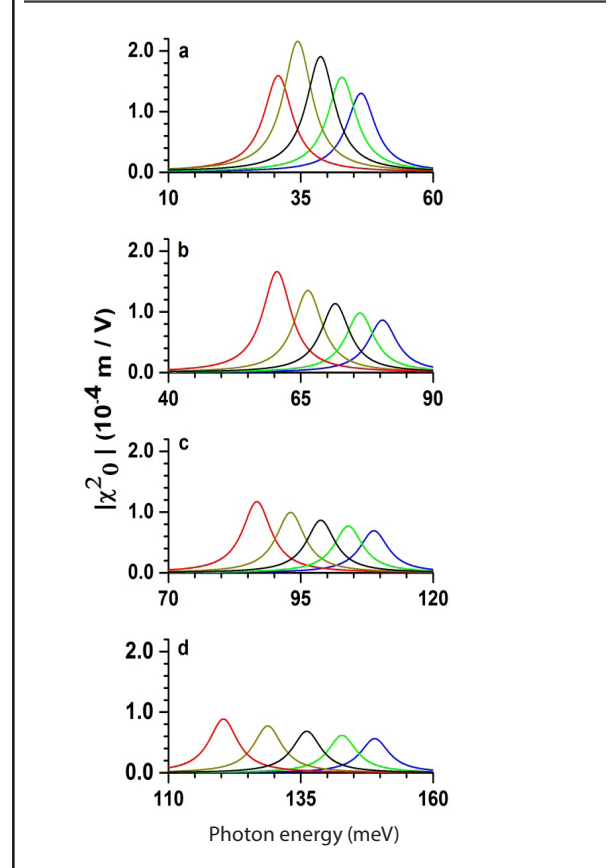
Figure 6. Confinement potential profiles, energies, and squares of the wave functions for the first two states in a Morse potential quantum well at (a) ($B = 5 \text{ T}$, $\gamma = 0.15 \text{ nm}^{-1}$) and (b) ($B = 20 \text{ T}$, $\gamma = 0.15 \text{ nm}^{-1}$).



The results of the nonlinear optical rectification as a function of the energy of the incident photons is presented in **Figures 7** and **8**. For the figures labeled with literal marks: in (a) $\gamma = 0,05 \text{ nm}^{-1}$, in (b) $\gamma = 0,10 \text{ nm}^{-1}$, in (c) $\gamma = 0,15 \text{ nm}^{-1}$ and in (d) $\gamma = 0,25 \text{ nm}^{-1}$. For the peaks shown in **Figure 1**, five electric field values are considered: -40 kV/cm (red), -20 kV/cm (ochre), $F=0$ (black), 20 kV/cm (green), 40 kV/cm (blue). When we compare **Figures 7a**, **7b**, **7c**, and **7d** we observe that the effect of the increase in parameter γ on the nonlinear optical rectification is to cause the peaks to move toward greater energy values, commonly called a blueshift. This is due to the fact that the transmission energy increases. When parameter γ increases, the effective width decreases, which can be observed by comparing **Figures 2a** and **2b**, making the dipole matrix elements decrease. The effect this has on the nonlinear optical rectification is a decrease in the magnitude of the peaks. For their part, the effects of the electric field are observed first in the position of the peaks: for negative values of the electric field -20 kV/cm and -40 kV/cm, the peaks are located at low energy values (we say there is a redshift); when there is no electric field ($F=0$, black) we observe the peak in the center of each figure; and for positive electric fields, the peaks show a blueshift. This is due to the fact that, as explained above, the electric field modifies the height of the finite potential barrier of the right of the well. This behavior implies a decrease in the magnitude of the peaks since decreasing the effective width of the quan-

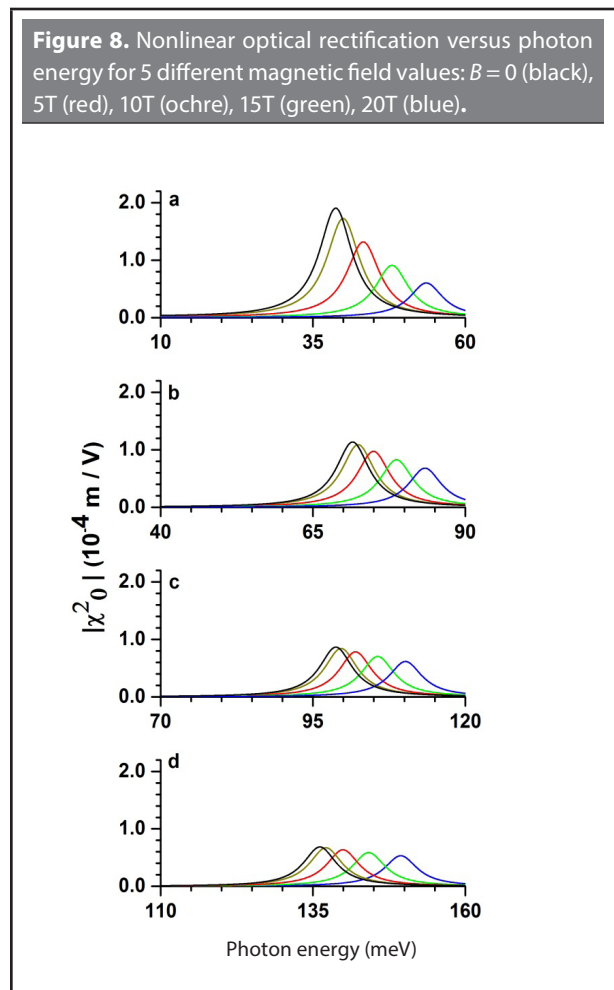
tum wells decreases the magnitude of the dipole matrix elements. This means that by changing parameter γ and the magnitude and direction of the electric field, we can adjust not only the position of the peak of the nonlinear optical rectification, but also its magnitude.

Figure 7. Nonlinear optical rectification versus photon energy for 5 values of electric field F : -40 kV/cm (red), -20 kV/cm (ochre), $F = 0$ (black), 20 kV/cm (green), 40 kV/cm (blue).



At the peaks of the nonlinear optical rectification in **Figure 8**, 5 magnetic field values are considered: $B = 0$ (black), 5T (red), 10T (ochre), 15T (green), 20T (blue). In this case, the nonlinear optical rectification also undergoes a blueshift, but here the change in the peak position is not equidistant, as in the situation shown in **Figure 7**. This is evident, for example, when comparing **Figures 7d** and **8d**. In addition, the magnitude of the peaks decreases as the magnetic field magnitude increases. The reason for this non-equidistant behavior in the location of the peaks of the optical response is easy

to understand through the observation of the energy difference between the states when the magnetic field reported in **Figures 5** and **6** is increased.



Regarding the perspectives of this study and given that this type of potential is obtained by graduating the aluminum concentration, one would expect that the profile of the valence band would also be Morse with confined states for gaps. This means that such a system would allow for transitions between these bands—conduction and valence—and intersubband transitions in the valence band. This study is restricted to the transitions between the first two states of the conduction band. In the study by Ramírez *et al.* (2011), an interesting discussion is presented of the formation of energy bands in a Gaussian AlGaAs quantum well, which consists of a non-homogeneous region where there aluminum concentration varies following a Gauss-

ian function, interspersed between two homogenous semi-infinite barriers with the fixed concentration of aluminum (which is the reference concentration) along the growth direction. Another interesting discussion is presented in the article by Oubram *et al.* (2014) that deals with the matter of light polarization for each type of transition possible in quantum Wells with delta-doped potentials. In particular, the peaks of the optical properties studied there can be distinguished using light with polarization perpendicular to the plane of the quantum well for intersubband transitions. On the other hand, the peaks related to the intersubband transitions can be favored when the light is polarized parallel to the plane of the quantum well. In this study, the polarized light is treated such that intersubband transitions are favored.

4. CONCLUSIONS

In this article, we studied the energies of the first two states of a semiconductor quantum well with a Morse potential profile. We analyzed transitions energies, dipole matrix elements, and nonlinear optical rectification under the combined effects of confinement parameter γ and the electric and magnetic fields. In general, confinement parameter γ makes the potential asymmetrical with a narrower and deeper quantum well effective width such that the state energy and transition energy increase. The position of the peaks in the nonlinear optical rectification show a blueshift and decrease in magnitude. The electric and magnetic fields produce similar effects, strengthening the asymmetry between the potential barriers and in the probability density. When the magnitude of any of them decreases, the value of the dipole matrix elements and the transition energies change. The peaks of the optical response studied undergo a blueshift for positive electric fields and a redshift for negative values; there are always blueshifts for growing magnetic fields. We can finally conclude that the combined effects of the confinement parameter and the electromagnetic fields can be used to adjust and control the optical properties of interest.

ACKNOWLEDGEMENTS

The authors thank the following Colombian institutions: CODI-Universidad de Antioquia (Sustainability

Strategy or *Estrategia de Sostenibilidad* of Universidad de Antioquia and the projects: “On the way to development of new concepts of nanostructure-based THz laser” and “Optical properties of impurities, excitons, and molecules in self-assembled quantum dots” or “*Propiedades ópticas de impurezas, excitones y moléculas en puntos cuánticos autoensamblados*”), the Natural Science Faculty of Universidad de Antioquia (CAD and ALM full-time project 2015-2016), and the Autonomous Patrimony National Fund for Financing Science, Technology and Innovation (*El Patrimonio Autónomo Fondo Nacional de Financiamiento para la Ciencia, la Tecnología y la Innovación*) Francisco José de Caldas, the EIA-UdeA Project (Intense Laser Effects on the Optical Properties of InGaAsN/GaAs and GaAlAs/GaAs Semiconductor Nanostructures or *Efectos de láser intenso sobre las propiedades ópticas de nanoestructuras semiconductoras de InGaAsN/GaAs y GaAlAs/GaAs*), which is partially financed by Universidad EIA, and the EIA’s Semiconductor Nanostructures Study Group (*Semillero de Nanoestructuras Semiconductoras*).

REFERENCES

- Barseghyan Manuk G.; Restrepo Ricardo L.; Mora-Ramos Miguel E.; A. Kirakosyan Albert and Duque Carlos A. (2012). Donor impurity-related linear and nonlinear intraband optical absorption coefficients in quantum ring: effects of applied electric field and hydrostatic pressure. *Nanoscale Research Letters* 7, pp. 538-1 – 538-8.
- Baskoutas S.; Garoufalis C.; Terzis A. F. (2011). Linear and nonlinear optical absorption coefficients in inverse parabolic quantum wells under static external electric field. *European Physics Journal B* 84, pp. 241 – 247.
- Bhattacharya P.; Mi Z. (2007). Proceedings of the Quantum-Dot Optoelectronic Devices IEEE 95, pp. 1723 – 1740.
- Castro E.; Paz J. L.; Martín P. (2006). Analytical approximations to the eigenvalues of the Morse potential with centrifugal terms. *Journal of Molecular Structure: THEOCHEM*. 769, Is. 1–3, pp. 15 – 18.
- Duque C. A.; Mora-Ramos M. E.; Kasapoglu E.; Ungan F.; Yesilgul U.; Sakiroglu S.; Sari H.; Sökmen I. (2013). Impurity-related linear and nonlinear optical response in quantum-well wires with triangular cross section. *Journal of Luminescence* 143, pp. 304 – 313.
- Guo A.; Du J. (2013). Linear and nonlinear optical absorption coefficients and refractive index changes in asymmetrical Gaussian potential quantum wells with applied electric field. *Superlattices Microstructures* 64, pp. 158 – 166.
- Gurnick M. K. and Detemple T. A. (1983). Synthetic nonlinear semiconductors. *IEEE Journal of Quantum Electronics*, QE-19, No. 5, pp. 791 – 794.
- Hargreaves, S.; Radhanpura, K.; Lewis, R. A. (2009). Generation of terahertz radiation by bulk and surface optical rectification from crystal planes of arbitrary orientation. *Physical Review B* 80, 195323-1 – 195323-16.
- Hayrapetyan D. B.; Kazaryan E. M.; Kotanjyan T. V.; Tevosyan H. K. (2015). Exciton states and interband absorption of cylindrical quantum dot with Morse confining potential. *Superlattices Microstructures* 78, pp. 40 – 49.
- Ikhdaïr S. M.; (2009). Rotation and vibration of diatomic molecule in the spatially-dependent mass Schrödinger equation with generalized q-deformed Morse potential. *Chemistry Physics* 361, pp. 9 – 17.
- Keshavarz A.; Karimi M. J. (2010). Linear and nonlinear intersubband optical absorption in symmetric double semi-parabolic quantum wells. *Physics Letters A* 374, pp. 2675 – 2680.
- Kumar M.; Lahon S.; Jha P. K.; Gumber S.; Mohan M. (2014). Spin-orbit interaction effect on nonlinear optical rectification of quantum wire in the presence of electric and magnetic fields. *Physica B: Condensed Matter* 438, pp. 29 – 33.
- Larrabee, D. C.; Tang, J.; Liang, M.; Khodaparast, G. A.; Kono, J.; Ueda, K.; Nakajima, Y.; Suekane, O.; Sasa, S.; Inoue, M.; Kolokolov, K. I.; Li, J.; Ning, C. Z. (2002). Intersubband transitions in narrow InAs/AlSb quantum wells. *Proceedings IEEE Lester Eastman Conference on High Performance Devices*, pp. 324 – 333.
- Lee H. J.; Juravel L. Y.; Woolley J. C. and Thorpe A. J. S. (1980). Electron transport and band structure of Ga_{1-x}Al_xAs alloys. *Physics Review B* 21, pp. 659 – 669.
- Lee, J.; Tymchenko, M.; Argyropoulos, C.; Chen, P.-Y.; Lu, F.; Demmerle, F.; Boehm, G.; Amann, M. -C.; Alu, A.; Belkin, M. A. (2014). Giant nonlinear response from plasmonic metasurfaces coupled to intersubband transitions. *Nature Letters* 511, pp. 65 – 69.
- Nakai, M.; Sasa, S.; Nakajima, Y.; Furukawa, M.; Inoue, M.; Larrabee, D. C.; Kono, J.; Li, J.; Ning, C. Z. (2004). Near infrared intersubband transitions in delta-doped InAs/AlSb multi-quantum wells. *International Meeting for Future of Electron Devices*, pp. 65 – 66.
- Oubram, O.; Rodríguez-Vargas, I.; Martínez-Orozco, J. C. (2014). Refractive index changes in n-type delta-doped GaAs under hydrostatic pressure. *Rev. Mex. Fis.* 60, pp. 161 – 167.

- Ramírez-Morales, A.; Martínez-Orozco, J. C.; Rodríguez-Vargas, I. (2011). Improvement of the quantum confined Stark effect characteristics by means of energy band profile modulation: The case of Gaussian quantum wells. *J. App. Physics* 110, pp. 103715-1 – 103715-6.
- Restrepo R. L.; Ungan F.; Kasapoglu E.; Mora-Ramos M. E.; Morales A. L. and Duque C. A. (2015). The effects of intense laser field and applied electric and magnetic fields on optical properties of an asymmetric quantum well. *Physica B: Condensed Matter* 457, pp. 165 – 171.
- Rosencher E. and Bois Ph. (1991). Model system for optical nonlinearities: Asymmetric quantum wells. *Physics Review B* 44, pp. 11315 – 11327.
- Rowley, J. D.; Wahlstrand, J. K.; Zawilski, K. T.; Schunemann, P. G.; Giles, N. C.; Bristow, A. D. (2012). Terahertz generation by optical rectification in uniaxial birefringent crystals. *Opt. Express* 15 (21), pp. 16968 – 16973.
- Shojaei S.; Vala A. S. (2015). Nonlinear optical rectification of hydrogenic impurity in a disk-like parabolic quantum dot: The role of applied magnetic field. *Physics E: Low-Dimensional System and Nanostructures* 70, pp. 108 – 112.
- Ungan F.; Kasapoglu E.; Sökmen I. (2011). Intersubband optical absorption coefficients and refractive index changes in modulation-doped asymmetric double quantum well. *Solid State Communications* 151, pp. 1415 – 1419.
- Ungan F.; Martínez-Orozco J. C.; Restrepo R. L.; Mora-Ramos M. E. and Duque C.A. (2015). Nonlinear optical rectification and second-harmonic generation in a semi-parabolic quantum well under intense laser field: Effects of electric and magnetic fields. *Superlattices and Microstructures* 81, pp. 26 – 33.
- Ungan F.; Restrepo R. L.; Mora-Ramos M. E.; Morales A. L.; Duque C. A. (2014). Intersubband optical absorption coefficients and refractive index changes in a graded quantum well under intense laser field: Effects of hydrostatic pressure, temperature and electric field. *Physica B: Condensed Matter* 434, pp. 26 – 31.
- Unterrainer K.; Heyman, J. N.; Craig, K.; Galdrikian, B.; and Sherwin, M. S.; Campman, K.; Hopkins, P. F.; Gossard, A. C. (1996). Intersubband dynamics of asymmetric quantum wells studied by THz 'optical rectification' *Semicond. Sci. Technol.* 11, pp. 1591–1597.
- Vodopyanov, K. L.; Chazapisdag, V.; Phillipsdag, C.; Sungddag, B.; Harris, J. S. Jr. (1997). Intersubband absorption saturation study of narrow III-V multiple quantum wells in the 152.8–9 mm spectral range. *Semicond. Sci. Technol.* 12, pp. 708 – 714.
- Vodopyanov, K. L. (2008). Optical THz-wave generation with periodically-inverted GaAs. *Laser Photon. Rev.* 2(1-2), pp. 11 – 25.
- Xia J. -B.; Fan W. -J. (1989). Electronic structures of superlattices under in-plane magnetic field. *Physics Review B* 40, pp. 8508 – 8515.
- Xie W. (2014). Effect of an electric field on the nonlinear optical rectification of a quantum ring. *Physica B: Condensed Matter* 443, pp. 60 – 62.
- Zhang, J.; Bull, J. D.; Darcie, T. E. (2007). Microwave photonic signal detection using phase-matched optical rectification in an AlGaAs waveguide. *IEEE Photonics Technology Letters* 19, pp. 2012 – 2014.

TO REFERENCE THIS ARTICLE /
PARA CITAR ESTE ARTÍCULO /
PARA CITAR ESTE ARTIGO /

Martínez, V.; Castaño, C.; Giraldo, A.; González, J.P.; Restrepo, R.L.; Morales, A.L.; Duque, C.A. (2016). Morse Potential as a Semiconductor Quantum Wells Profile. *Revista EIA*, 12(E3), May, pp. 85-94. [Online]. Available on: <http://dx.doi.org/10.14508/reia.2016.12.e3.85-94>